Rotation and Curvature Correction Assessment for One- and Two-Equation Turbulence Models

M. Mani,* J. A. Ladd,† and W. W. Bower‡
The Boeing Company, Saint Louis, Missouri 63166

The rotation and curvature (RC) correction proposed by Spalart and Shur, as well as the RC correction proposed by Hellsten, have been implemented in the Wind code. Both models were applied to a subsonic flow in a U-turn duct and a high-speed ground/jet interaction. Both models performed well for the U-turn duct. The Spalart and Shur RC correction is more sophisticated and, therefore, more accurate, general, and computationally intensive than the RC correction proposed by Hellsten.

Nomenclature

C_f	=	skin-friction coefficient
C_{RC}	=	rotation and curvature correction factor
f_{r1}	=	rotation function
R_i	=	Richardson number
S_{ij}	=	strain tensor
t	=	time
ρ	=	density
ω	=	magnitude of vorticity

Introduction

FOR computational fluid dynamics (CFD) applications to be able to predict turbulent shear flows accurately, the turbulence model needs to account for streamline curvature and/or system rotation. Various corrections to account for streamline curvature and rotation have been introduced by different researchers in the past[1–4] and are applicable to the certain types of flows for which they were designed. To account for these phenomena, more complex turbulence models such as the Reynold-stress formulation were employed. Unlike eddy-viscosity models, the Reynolds stress models explicitly contain the rotation and curvature correction source term; however, these high-end models are too computationally intensive and not practical for routine engineering applications.

The rotation and curvature (RC) corrections of Refs. 5 and 6 have been implemented in the Wind code[7] and applied to two different applications. The objective is to assess their impact on complex flowfields with weak and strong streamline curvature.

Wind is a multizone, implicit, structured, compressible flow solver, which operates in two-dimensional, three-dimensional, and axisymmetric modes. The zonal interface may be overlapped or abutting. The overlapping capability allows complex systems to move relative to each other. Turbulence can be modeled by a variety of algebraic, one- and two-equation turbulence models. For most Wind applications, either the one-equation Spalart–Allmaras (S-A) model[8] or two-equation Menter Shear Stress Transport (SST) model[9] is used. These provide reasonable accuracy for attached and separated boundary layers, as well as for shear layers. Distributed parallel processing allows distribution of the solution to several processors and, therefore, reduces the computation time.

In this paper, we investigate subsonic flow through a highly curved surface and high-speed jet impinging on the ground. The former was run to validate the models against a well-established test case with experimental data. The latter is important in the understanding of the next-generation short takeoff and landing aircraft. These jets are highly unsteady and degrade the aircraft performance. These adverse effects are lift loss, sonic fatigue, and hot gas ingestion. For more detail on ground jet interaction see Ref. 10.

Rotation and Curvature Correction

Spalart and Shur[5] proposed a unified approach to account for streamline curvature and system rotation that is applicable to both one- and two-equation models. We have applied it to the one-equation Spalart–Allmaras turbulence model (SARC) and demonstrated it to be quite competitive with the advanced Reynold-stress turbulence models. Their approach is based on empirical data and intuitive arguments and is similar to that of Knight and Saffman, proposed in 1978 (Ref. 11). They both track the direction of the principal axes of the strain tensor and, thus, are coordinate invariant. However, the SARC differs from Knight and Saffman approach in many ways and, in particular, avoids the troublesome step of computing and numerically differentiating the principal direction. In addition, the SARC provides an explicit formula for the RC correction, and, therefore, it is easier to apply to three dimensions than is the formulation of Knight and Saffman.

The SARC approach involves second-order derivatives of the velocity field. This is in contrast to many of the previous approaches, including that of Hellsten,[6] that do not include these terms.

In terms of the one-equation S-A model, implementation leads to a fairly simple modification to the program equation set. Specifically, the source term $(C_{b1}\omega\tilde{\nu})$ is multiplied by the rotation function f_{r1}, where $\tilde{\nu}$ is the modified eddy viscosity. The rotation function is as follows:

$$f_{r1}(r^*,\tilde{r}) = (1+c_{r1})[2r^*/(1+r^*)]\bigl[1-c_{r3}\tan^{-1}(c_{r2}\tilde{r})\bigr]-c_r1 \quad (1)$$

where, r^* and $\tilde{r}$ are nondimensional quantities given by

$$r^* = \frac{S}{\omega}, \qquad \tilde{r} = 2\omega_{ik}S_{jk}\left(\frac{\mathrm{D}S_{ij}}{\mathrm{D}t}\right)\Big/D^4$$

$$S_{ij} = 0.5\left(\frac{\partial u_i}{\partial x_j}+\frac{\partial u_j}{\partial x_i}\right), \qquad \omega_{ij} = 0.5\left(\frac{\partial u_i}{\partial x_j}-\frac{\partial x_i}{\partial u_j}\right)$$

$$D^2 = \omega_{ij}^2 + S_{ij}^2$$

and $\mathrm{D}S_{ij}/\mathrm{D}t$ are the components of the Lagrangian derivative of the strain tensor. The constants of the model are $c_{r1}=12$, $c_{r2}=1.0$, and $c_{r3}=1.0$ as proposed by Spalart and Shur.[5]

For the two-equation SST turbulence model, Hellsten[6] presented a simpler approach for the RC correction. In this approach, the source term $\beta\rho\omega^2$ in the ω equation is multiplied by the function F_4. The function F_4 is constructed as follows:

$$F_4 = 1/(1 + C_{RC}R_i) \qquad (2)$$

Where R_i is calculated by the following equation:

$$R_i = (|\omega_{ij}|/|S_{ij}|)(|\omega_{ij}|/|S_{ij}| - 1) \qquad (3)$$

The value of the RC correction factor $C_{RC} = 3.6$ has been calibrated and proposed by the authors. It is found that this coefficient is not universal and requires adjustment for high-speed ground/jet interaction. The results obtained with $C_{RC} = 3.6$ are referred to as SSTRC and results with the modified $C_{RC} = 1.4$ are referred to as the modified SSTRC.

The preceding approaches have been validated in Refs. 6 and 12 for two-dimensional and three-dimensional low-speed applications. Both approaches perform well compared with the experimental data. The objective of this paper is to assess the accuracy of these methods for compressible flows with streamline curvature.

Results

Flow Through a U-Turn Duct

To validate and understand the basic effects of RC corrections on the S-A and SST turbulence models, the flow through a duct with a U-turn was run, and the results are compared against the data. The solution was obtained on a 289×161 grid. The grid is shown in Fig. 1, where only every third grid point is shown for clarity. The solution was obtained with a freestream Mach $= 0.2$, $Re/\text{ft} = 1.0 \times 10^6$ $Re/\text{m} = 3.28 \times 10^6$, and the outflow pressure set to freestream. The solution started from the uniform flow and was converged on three different grid resolutions (73×41, 145×81, and 289×161) to ensure grid-independent solutions.

Figures 2a–2d displays the particle traces through the duct with and without the RC corrections. The separation regions downstream of the turn shows that the separation region grows with the RC corrections. Velocity profiles are shown in Fig. 3 at four different locations: $\theta = 0.0$, 90.0, and 180, and $S/H = \pi + 2$. As expected, the results with the RC correction shown in Figs. 3c–3f match the data more closely than does the solution without the RC correction.

Figures 3a and 3b show the skin-friction and pressure coefficients along the outer boundary. The results obtained from the S-A and SST models without the RC corrections miss the C_f peak significantly. The SARC model predicts the surface pressure coefficient most accurately. In the downstream section, all models except the SARC over- or under-predict the data.

At $\theta = 0$ the velocity profiles from both models are very similar and match the data closely, except for the S-A model (Fig. 3c). At $\theta = 90$ and 180 (Figs. 3d and 3e), both RC corrections improve the velocity profile prediction, but SARC matches the data most accurately. After the separation at $S/H = \pi + 2$ (Fig. 3f), the results with the RC corrections significantly differ from the data. It appears that the RC correction causes the overprediction of the separation region and slows down the recovery from it (Figs. 2a–2d). Reference 13 indicates that this shortfall might be related to the turbulence model inaccuracies observed in plane flows with massive separation and reattachment. The RC correction[6] applied to the SST model has less of an impact on the recirculation region than does the RC correction[5] for the S-A model.
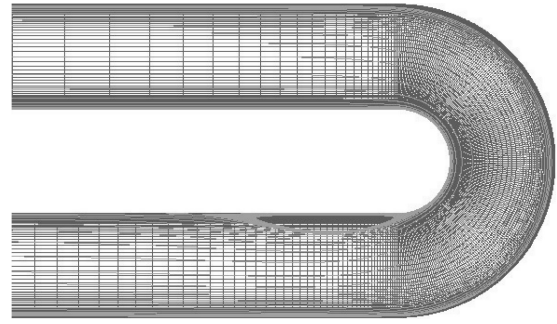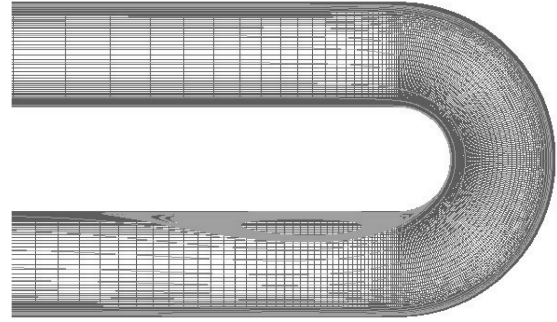
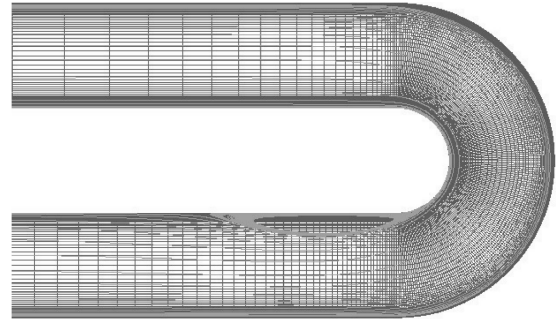**Fig. 2a Particle traces (S-A).**

Fig. 2b Particle traces (S-A-RC).
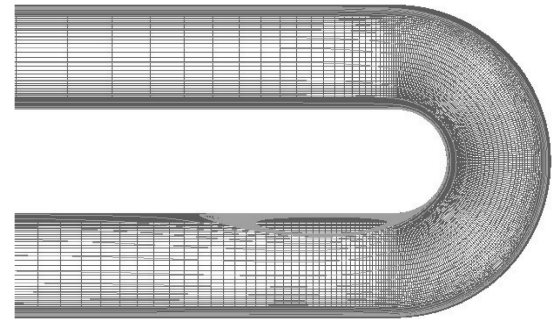
Fig. 2c Particle traces (SST).

Fig. 2d Particle traces (SSTRC).

Fig. 1 Two-dimensional grid (289×161) for the U-turn geometry; every third grid line is shown.
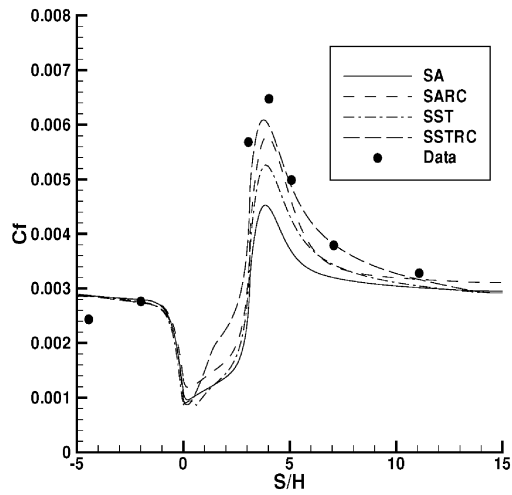
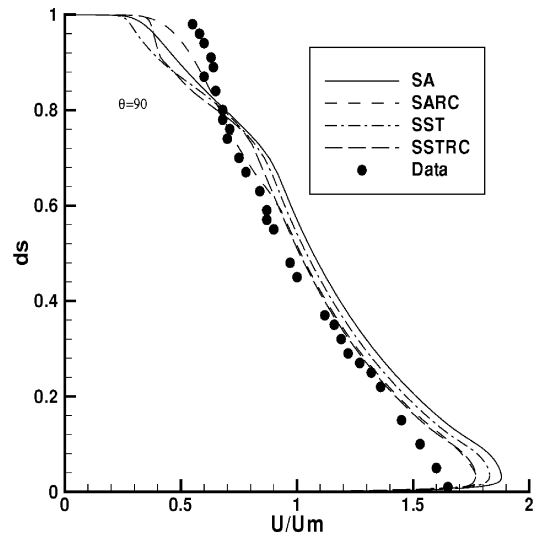Fig. 3a   Skin-friction coefficient along the outer surface.
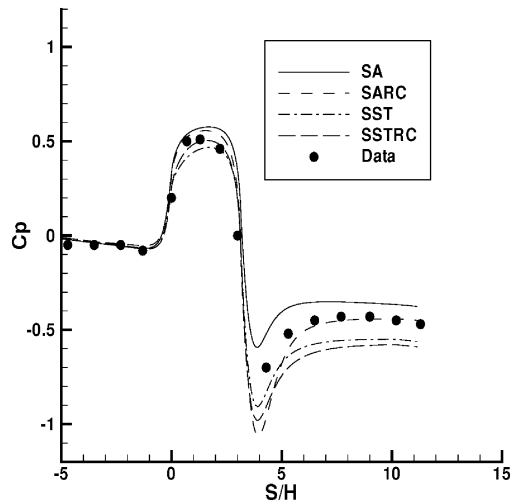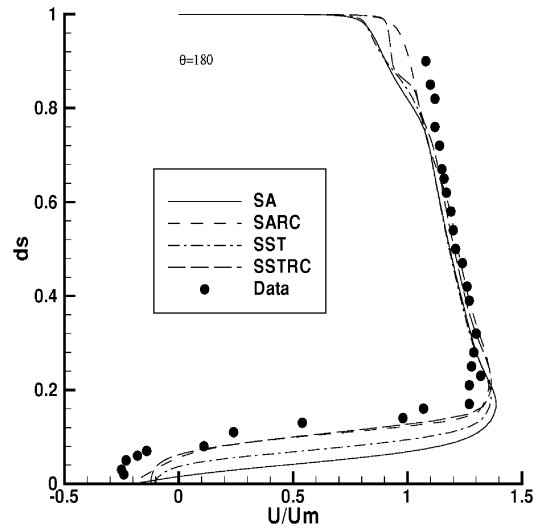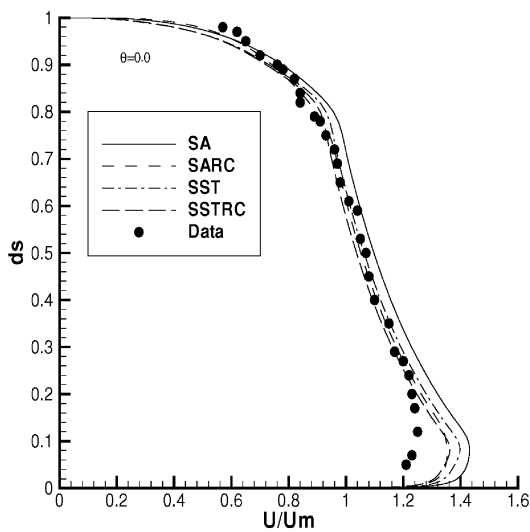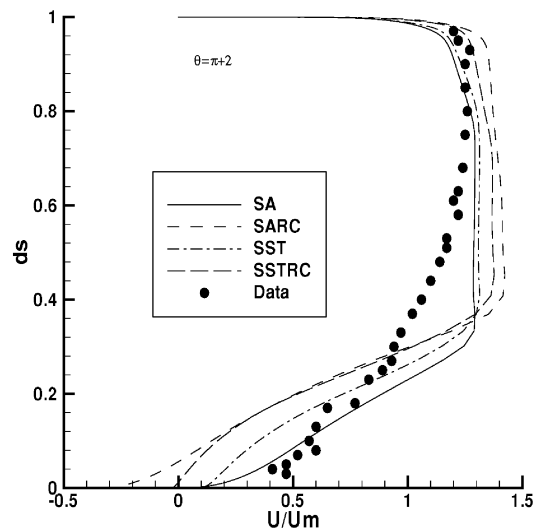

Fig. 3d   Velocity profile across the duct at $\theta = 90$.

Fig. 3b   Surfase pressure coefficient along the outer surface.

Fig. 3e   Velocity profile across the duct at $\theta = 180$.

Fig. 3c   Velocity profile across the duct at $\theta = 0$.

Fig. 3f   Velocity profile across the duct at $\theta = \pi + 2$.

Impinging Jet Flow

Two sets of time-accurate solutions were obtained for ground/jet interactions in the axisymmetric mode, to investigate the effects of the RC corrections for this type of flow. Initial attempts at using local time stepping caused the flowfield to become largely unsteady, and a converged steady-state solution was not possible. The time-accurate computation, although it required many more iterations, reduced the unsteadiness and allowed a time-averaged flowfield to be obtained. An axisymmetric grid plane containing five zones and 28,000 points was employed for this study. Both cases were run at a nozzle pressure ratio of 5 and a height-to-exit-diameter ratio (H/D) of 3. Both nozzles were convergent with a 4.7-in. exit diameter for the first case and a 1.0-in. exit diameter for the second. The freestream and jet stagnation conditions are as follows.

1) For case 1, freestream stagnation conditions, $M = 0.01$, $P = 14.7$ psi, and $T = 527$ R. For jet stagnation conditions, $M = 0.135$, $P_t = 73.5$ psi, and $T_t = 527.0$ R.

2) For case 2, freestream stagnation conditions, $M = 0.01$, $P = 14.62$ psi, and $T = 569.67$ R. For jet stagnation conditions, $M = 0.135$, $P_t = 73.08$ psi, and $T_t = 2260$ R.

The grid in the vicinity of the jet impingement is shown in Fig. 4. Only every other point is displayed for clarity. The Mach contours for the S-A and SARC are show in Fig. 5. The flow accelerates outside the nozzle to Mach 2.8. As the flow approaches the ground, a Mach disk is formed, and the flow becomes subsonic in a recircu-

lating region near the jet centerline. Figure 6 shows the streamline traces for the S-A and SST turbulence models with and without the RC corrections. Accurate prediction of the recirculation region is essential for accurate prediction of the surface pressure and the location of the Mach disk. Different turbulence models predict the width and height of the recirculation region differently. As shown in Fig. 7 the size of the recirculation zone predicted by the SST and SARC agree closely with the experiment.
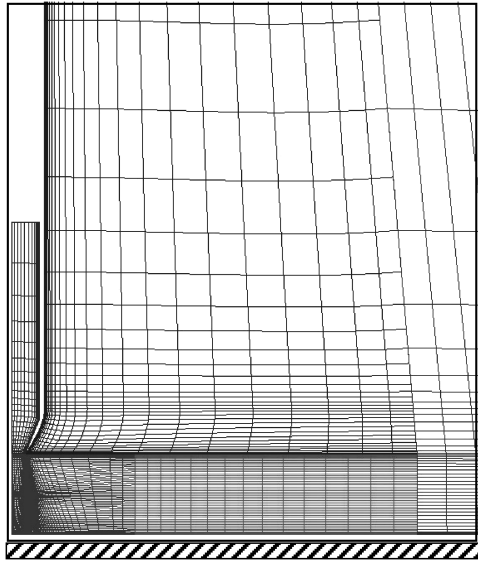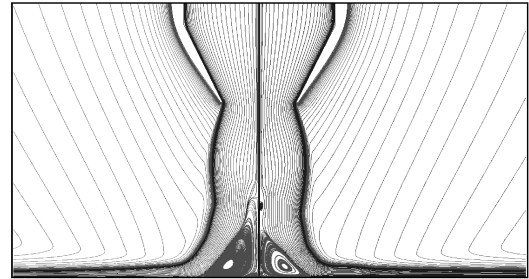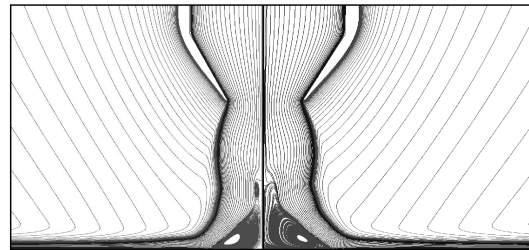

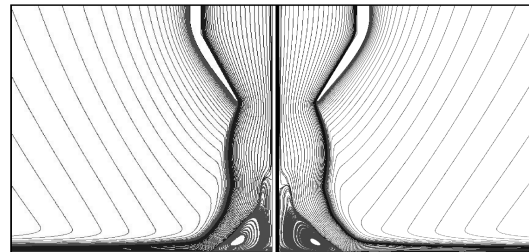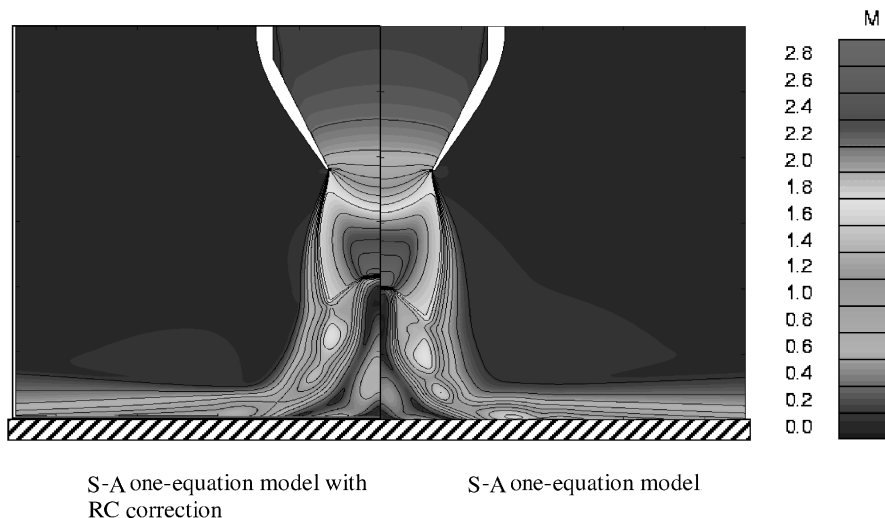SA-RC   S-A

SSTRC   SST

Modified SSTRC   SST

Fig. 6   Computed mean streamline traces for case 1.

Fig. 4   Axisymmetric grid for ground/jet interaction; every other point shown here.

S-A one-equation model with   S-A one-equation model
RC correction

Fig. 5   Mach contours for case 1.

A comparison of total velocity contours from experiment and those computed from the S-A, SARC, SST, SSTRC, and modified SSTRC turbulence models are shown in Fig. 7. The plots in Fig. 7 have been distorted (expanded y axis) to show the details of the flow structure. The results of SARC and modified SSTRC compare well with the experimental data in terms of the Mach disk location and the size of the recirculation region. However, both RC corrections introduce a higher total velocity in the core near the ground, which is not seen in the experimental results.

The time-averaged normalized pressure Cp_2 on the ground plane vs radial distance is shown in Fig. 8a for case 1 (Ref. 14). The normalized pressure Cp_2 is the ratio of $(p - p_{inf})/(p_{tj} - p_{inf})$. The S-A model without the RC correction significantly overpredicts the surface pressure in the impingement region. In this simulation, the SARC and SST results are very similar and match the data closely, although they are slightly high near the jet centerline. The RC correction proposed by Hellsten[6] (with $C_{RC} = 3.6$) has an adverse effect on the prediction with the SST model, and the results deviate from the experiment for the ground/jet interaction. This is mainly due to the excessive turbulent viscosity produced in the ground's vicinity where the jet shear layer impinges on the ground. Reduction of the C_{RC} to 1.4 provides a much more accurate pressure on the ground (shown in Fig. 8a as SSTRC2). This model has a different effect on the results depending on the value of the C_{RC}. One can conclude that the value of C_{RC} is not universal. This is not surprising because this is a less sophisticated modeling of the RC correction.

Figure 8b depicts the results for the case 2 (Ref. 15) nozzle study. This case was run only with the S-A turbulence model with and without the RC correction. The SARC results agree well with the experiment. It appears that the RC correction proposed by Spalart and Shur[5] has a significant and consistent effect on flows with streamline curvature for both cold and hot jets.

Figure 9 compares the contours of the density gradient for case 1 with SARC vs the shadowgraph of the experiment from Ref. 10. Most of the flow characteristics have been accurately captured in the numerical solution. However, the location of the Mach disk is slightly lower than shown in the shadowgraph.
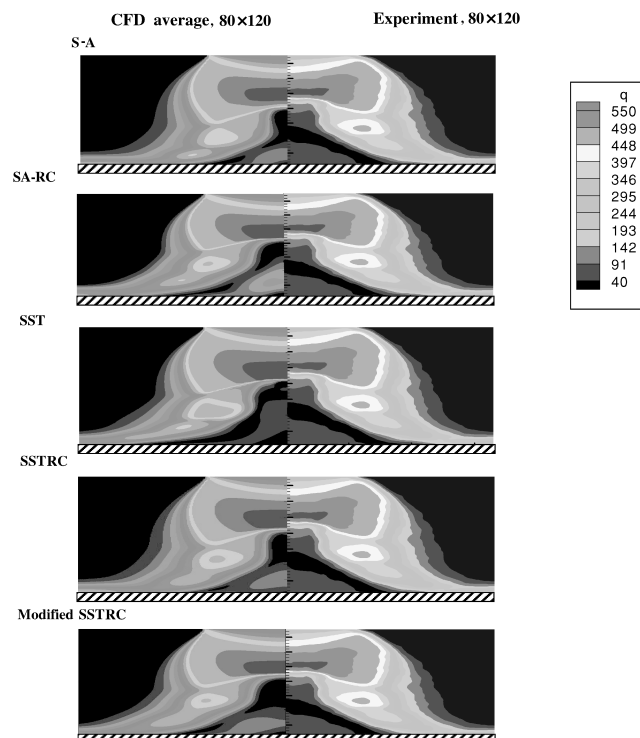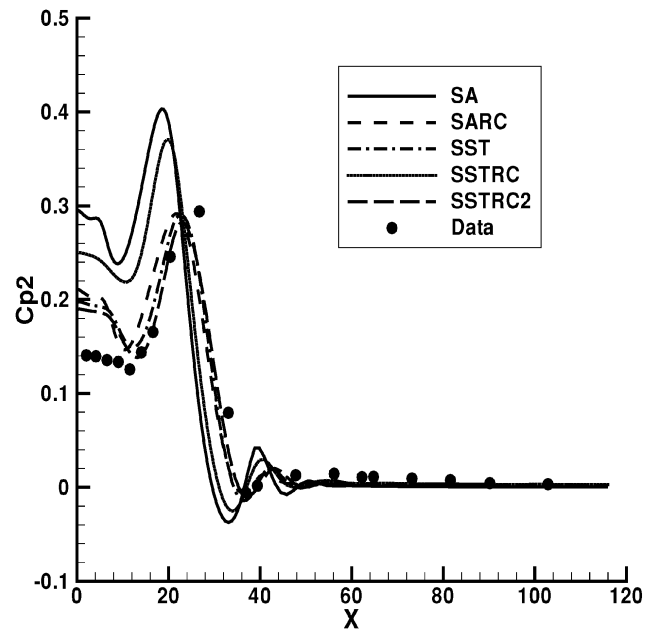

Fig. 8a   Surface pressure coefficient comparisons (case 1).
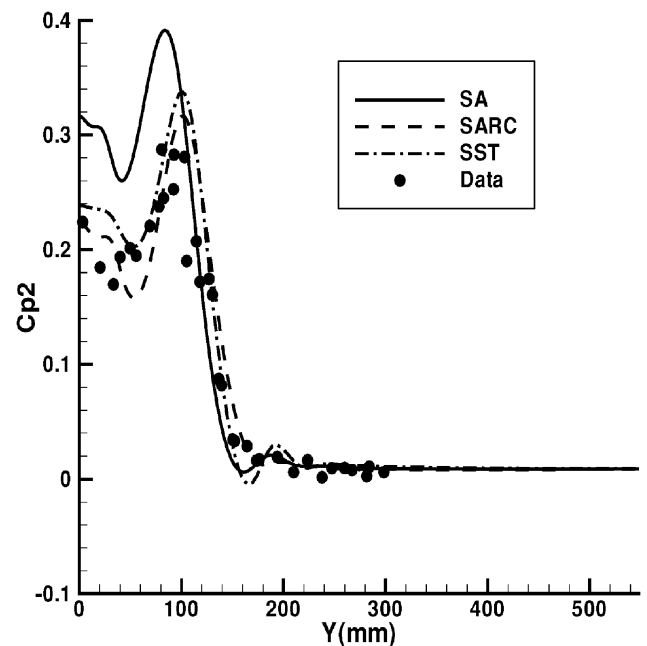
Fig. 8b   Surface pressure coefficient comparisons (case 2).

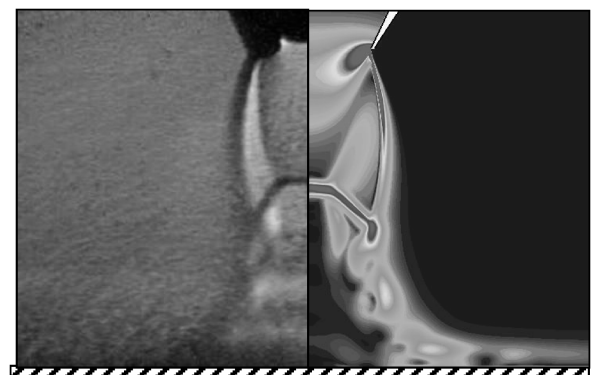Fig. 7   Total velocity for case 1 (distorted).

Fig. 9   Shadowgraph vs computed density gradient contours.

Conclusions

The RC corrections developed by Spalart and Shur[5] and Hellsten[6] have been applied to two different flows with streamline curvatures. The results have consistently been improved with the approach proposed in Ref. 5. The approach proposed in Ref. 6 has demonstrated somewhat mixed results. The results obtained for ground/jet interaction cases indicate that the one-equation SARC model behaves very similarly to the baseline two-equation SST model. To further improve the SARC results, a compressibility correction and turbulent treatment for unsteady separated flow Detached Eddy Simulation (DES) should be applied. The RC correction proposed by Hellsten[6] requires further improvement to be applicable to complex high-speed cases. The CPU/node/iteration increases by 9.5% to compute the RC correction of Spalart and Shur and only 2.6% for the Hellsten corrections.

References

[1]Launder, B. E., Priddin, C. H., and Sharma, B. I., "The Calculation of Turbulent Boundary Layers on Spinning and Curved Surfaces," *Journal of Fluids Engineering*, Vol. 99, 1977, pp. 231–239.

[2]Park, S. V., and Chung, M. K., "Curvature-Dependent Two-Equation Model for Prediction of Turbulent Recirculating Flows," *AIAA Journal*, Vol. 27, No. 3, 1989, pp. 340–344.

[3]Gillis, J. C., and Johnston, J. P., "Turbulent Boundary Layer Flow and Structure on a Convex Wall and Its Redevelopment on a Flat Plate," *Journal of Fluid Mechanics*, No. 135, 1983, pp. 123–153.

[4]Bradshaw, P., and Castro, I. P., "The Turbulence Structure of a Highly Curved Mixing Layer," *Journal of Fluid Mechanics*, No. 73, Pt. 2,

1976, pp. 265–304.

[5]Spalart, P. R., and Shur, M. L., "On the Sensitization of Turbulence Models to Rotation and Curvature," *Aerospace Science and Technology*, Vol. 1, No. 5, 1997.

[6]Hellsten, A., "Some Improvements in Menter's k–ω SST Turbulence Model," AIAA Paper 98-2554, 1998.

[7]Bush, R. H., Power, G. D., and Towne, C. E., "Wind: The Production Flow Solver of the NPARC Alliance," AIAA Paper 98-0935, Jan. 1998.

[8]Spalart, P. R., and Allmaras, S. R., "A One-Equation Turbulence Model for Aerodynamic Flows," AIAA Paper 92-0439, Jan. 1992.

[9]Menter, F. R., "Zonal Two-Equation k–ω Turbulence Models for Aerodynamic Flows," AIAA Paper 93-2906, July 1993.

[10]Alvi, F. S., and Ladd, J. A., "Experimental and Numerical Investigation of Supersonic Impinging Jets," AIAA Paper 2000-2224, June 2000.

[11]Knight, D. D., and Saffman, P. C., "Turbulence Model Predictions for Flows with Significant Mean Streamline Curvature," AIAA Paper 78-258, 1978.

[12]Shur, M., Strelets, M., Travin, A., and Spalart, P. R., "Turbulence Modeling in Rotating and Curved Channels: Assessment of the Spalart-Shur Correction Term," AIAA Paper 98-0325, 1998.

[13]Shur, M., Spalart, P. R., "Comparative Numerical Testing of One- and Two-Equation Turbulence Models for Flows with Separation and Reattachment," AIAA Paper 95-0863, 1995.

[14]Alvi, F. S., and Iyer, K. G., "Mean and Unsteady Flowfield Properties of Supersonic Impinging Jets with Lift Plates," AIAA Paper 99-1829, 1999.

[15]Angel, R. G. A., "JSF Surface Erosion Materials Characterisation Program Test Results," Internal Rept. FAE-R-RES-4620, Issue 1, British Aerospace PLC, April 1999.